MICROMECHANICAL MODELLING OF FRP-STRENGTHENED CONCRETE STRUCTURES

Kenneth W. NEALE [a], Hussien ABDEL BAKY [b], Abdallah YAHIAOUI [b], Usama A. EBEAD [c]

[a] Prof.; Université de Sherbrooke, 2500, boul. de l'Université, Sherbrooke, Québec, Canada J1K 2R1
E-mail address: *Kenneth.Neale@USherbrooke.ca*

[b] Dr.; Université de Sherbrooke, 2500, boul. de l'Université, Sherbrooke, Québec, Canada J1K 2R1
E-mail address: *Hussien.El.Baky@USherbrooke.ca, Abdallah.Yahiaoui@USherbrooke.ca*

[c] Assistant Prof.; United Arab Emirates University, Al Ain, United Arab Emirates,
E-mail address: *Uebead@uaeu.ac.ae*

Received: 10.11.2009; Revised: 15.01.2010; Accepted: 17.02.2010

Abstract

In this study, micromechanics-based finite element simulations of FRP-strengthened concrete structures are presented. This paper first focuses on three main simulations. In the first application, 3D nonlinear micromechanics-based finite element analyses are performed to investigate the interfacial behaviour of FRP/concrete joints subjected to direct shear loadings. The finite element modelling of FRP-strengthened concrete beams are presented in the second simulation to capture the debonding loads. Finally, the confining behaviour of FRP-wrapped concrete columns is investigated. An accurate equation correlating the axial stiffness of the FRP laminates and the lateral strain of the concrete columns to the lateral confining pressure is incorporated in the code to predict the behaviour up to failure. Furthermore, this application is reanalysed using 3D FE models. Minor discrepancies are observed between the two predictions.

In the second part of the paper, numerical comparisons are presented between the predictions of a phenomenological concrete constitutive law (hypoelastic relations with a smeared crack model) and the micromechanics-based analysis (microplane theory) to simulate the concrete behaviour in the three applications. The FE analyses are carried out using 8-node 3D solid elements for the concrete and 4-node orthotropic shell elements for the FRP laminates. A high performance parallel computing technique that employs supercomputers is used for carrying out the analyses to accommodate the computational demands of running the simulations.

Streszczenie

W artykule przedstawiono bazujące na mikromechanice materiałów symulacje MES elementów betonowych wzmocnionych FRP. W artykule skoncentrowano się na trzech głównych symulacjach. W pierwszej, trójwymiarowe, nieliniowe analizy MES bazujące na mikromechanice materiałów wykonano aby zbadać zachowanie się w płaszczyźnie styku połączenia materiału FRP i betonu poddanego obciążeniu ścinającemu. W drugiej symulacji przedstawiono modele MES betonowych belek wzmocnionych FRP w celu uchwycenia obciążenia delaminującego. Na koniec przedstawiono badania zachowania się słupów betonowych owiniętych FRP. Dokładny wzór korelujący osiową sztywność laminatów FRP i poprzeczne odkształcenie betonowych słupów do poprzecznego naporu ograniczającego został wprowadzony do programu aby przewidywać zachowanie aż do zniszczenia. Co więcej, zastosowanie to zostało ponownie przeanalizowane przy użyciu trójwymiarowych modeli MES. Zaobserwowano niewielkie rozbieżności pomiędzy tymi dwoma podejściami.

W drugiej części artykułu przedstawiono numeryczne porównania pomiędzy podejściem fenomenologicznym prawa konstytutywnego betonu (hyposprężyste związki z modelem rysy rozmytej) i analizy bazującej na mikromechanice materiałów (teoria mikropłaszczyzn) do symulacji zachowania się betonu w trzech zastosowaniach. Analizy MES zostały przeprowadzone przy użyciu trójwymiarowych, 8-węzłowych elementów bryłowych dla betonu i 4-węzłowych, ortotropowych elementów powłokowych dla laminatów FRP. Wysoka wydajność równolegle z techniką obliczeniową, którą stosują superkomputery zostały wykorzystane do przeprowadzenia analiz dostosowując wymagania obliczeniowe przeprowadzanych symulacji.

Keywords: **Microplane; FRP-strengthened beams; Direct shear test; FRP-wrapped columns.**

1. INTRODUCTION

Over the years, there has been considerable interest in the constitutive modeling of brittle-plastic materials such as concrete. Essentially two approaches have been employed; namely, the phenomenological and the micromechanics-based models. The former have been inspired by the classical macroscopic theories of plasticity and damage. These relations are developed based on the hypotheses and assumptions observed experimentally for the macroscopic response of concrete. On the other hand, micromechanics-based constitutive laws of concrete, such as the microplane concrete theories, focus primarily on microscopic phenomena, such as microcrack formation at mortar-aggregate interfaces. The macroscopic responses therefore arise from what occurs at the microscopic level.

Two groups of micromechanics-based constitutive laws have been employed in the finite element simulations of the concrete structures. The first approach, referred to as the "microplane model", was developed based on concepts in the slip theory of plasticity previously proposed by Batdorf and Budiansky [1]. The material element here represents the heterogeneous microstructure of concrete in a smeared manner where each microplane represents the damage or weak plane at the microstructural level, such as contact layers between the aggregate pieces in the concrete [2, 3]. The random structure of aggregates inside the concrete at the mesoscopic level is taken into consideration in the second micromechanical approach, referred to as the "mesoscale model" [4, 5]. These models demand an enormous computational capacity when large structures are simulated. In general, this approach is used to investigate the effect of the microstructure composition such as aggregate shape and size on the mechanical responses of the concrete.

This study will focus only on the microplane concrete model as a constitutive law in simulating the microstructural response of FRP-strengthened concrete structures. Consequently, considerable efforts have been devoted in this work to formulate the constitutive relations of the model and to implement the formulation in a finite element package, ADINA 8.4 [6] as a user-defined subroutine. To our knowledge, this work constitutes the first attempt to use the microplane model, as a concrete constitutive law, for simulating the microstructural behaviour of FRP-strengthened concrete structures.

In the finite element simulations of FRP-strengthened concrete structures, the constitutive laws to date have been almost exclusively phenomenological in nature. Although the macroscopic constitutive relations together with a cracking model is accepted and accurate for a wide range of applications, they have been proven inadequate in providing unified constitutive relations that accurately reflect the experimental data for arbitrary deformation histories for concrete. For example, the shear response of the cracked concrete is simulated using an empirical shear retention factor based on the tensile principal strain value regardless of the interaction of the other two principal strain values. This model is incapable of capturing the shear nonlinearity of the concrete or accounting for the shear-compression interaction [7]. In the same manner, a survey of the literature reveals that two basic phenomenological constitutive relations have been broadly adopted to analytically model the concrete behaviour under compressive state of stress; namely, elasticity and plasticity formulations [8, 9]. Each of these approaches can well describe some features of the concrete behaviour, while the other features are poorly represented [10, 11, 7, 12, 9]. The lateral dilation of the concrete and the associated softening behaviour is represented in the elasticity-based relations. However, these models fail to account for the confinement effect. On the other hand, the hardening plasticity theory has been adopted in several studies to capture the effect of high confinement on the behaviour of concrete; however, it has not been able to simulate the softening and cracking responses in case of relatively low confinement pressures [13]. On the other hand, the microplane concrete hypothesis has proven to be very effective in representing the behaviour of concrete under a wide range of complex stress and strain histories [2, 3].

The absence of simulations of FRP-strengthened concrete structures using micromechanics-based models is undoubtedly a result of computational demands of these analyses. With the advent of supercomputers over the last few years, researchers are now able to apply micromechanics-based models and use a very large number of discrete finite elements. The supercomputer employed for this research, known as "Mammoth", is the most powerful parallel supercomputer in Canada. It is at the University of Sherbrooke and consists of 576 nodes with a maximum speed of 4147.2 GHz. Each node consists of two processors of 3.6 GHz with a total RAM of 8.0 GB.

Within the framework of this paper, a brief summary of the basic relations of the M4 version of the microplane model is first given. This includes a sum-

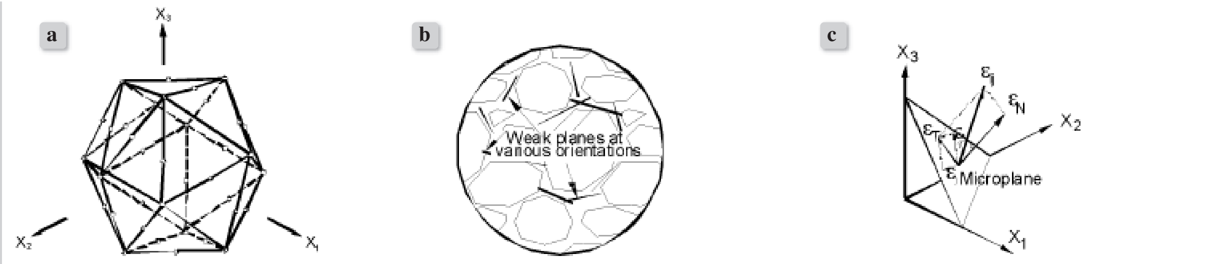

(a) Spatial distribution of microplanes (b) Weak planes at microstructure (c) decomposition of strain level tensor on a microplane

Figure 1.
Unit volume of microplane model

mary of the main features of the user-defined subroutine. We then present the finite element models. Three applications of FRP-strengthened concrete structures are considered; namely, FRP/concrete joints, reinforced concrete beams strengthened in flexure with FRPs and FRP-wrapped concrete columns. Finally, to demonstrate the efficiency of the microstructural simulations of FRP-strengthened concrete structures, we apply the hypoelastic concrete model to carry out the three applications mentioned above. This exercise serves to demonstrate the accuracy of micromechanics-based finite element simulations in these applications.

2. REVIEW OF THE MICROPLANE CONCRETE MODEL M4

Two different concrete constitutive laws have been employed in the numerical simulations to represent the concrete characteristics. The first is the microplane concrete model detailed below, while the second is the hypoelastic formulations available in the ADINA software. A special emphasis at the end of the paper assesses the abilities of the two constitutive relations in the three different applications.

Full details concerning the underlying hypotheses, basic relations, and inherent advantages as well as difficulties of the M4 version of the microplane model can be found in Bažant et al. [3] and Caner and Bažant [14]. A brief recapitulation of its main features is presented below.

With this constitutive theory, a representative volume of material is viewed at the microstructural level, and is considered as a three-dimensional element defined by a set of microplanes of different orientations arranged in a regular pattern. A typical representation is shown in Figure 1(a), which depicts a material element characterized by 28 equally-distributed planes per hemisphere. These planes represent the damage or weak planes at the microstructural level (aggregate-mortar interface) or planes of microcrack formation as depicted in Figure 1(b). The orientation of each plane is specified by a unit normal vector, having components n_i. The key assumption in the theory is that the macroscopic strain tensor, ε_{ij}, can be projected into a microscopic normal strain vector ε_N and shear strain vector ε_T on each microplane as illustrated schematically in Figure 1(b). The normal vector is given by:

$$\varepsilon_N = N_{ij}\varepsilon_{ij} \tag{1}$$

where $N_{ij} = n_i n_j$. To better control the triaxial behaviour, Bažant and Prat (1988) have proposed splitting this vector into volumetric ε_V, and deviatoric ε_D strain vectors; i.e.,

$$\varepsilon_N = \varepsilon_V + \varepsilon_D \tag{2}$$

The volumetric component characterizes the hydrostatic behaviour of the concrete; it is considered an invariant, such that [16]:

$$\varepsilon_V = \frac{\varepsilon_{ij}\delta_{ij}}{3} \tag{3}$$

where δ_{ij} is the Kronecker delta. With regard to the microscopic shear strain component ε_T, it is further decomposed into two components with respect to perpendicular directions l and m in the plane as follows:

$$\varepsilon_M = M_{ij}\varepsilon_{ij}, \quad \varepsilon_L = L_{ij}\varepsilon_{ij} \tag{4}$$

where $M_{ij} = (m_i n_j + m_j n_i)/2$ and $L_{ij} = (l_i n_j + L_j n_i)/2$. The magnitude of ε_T is given by:

$$\varepsilon_T = \sqrt{\varepsilon_L^2 + \varepsilon_M^2} \tag{5}$$

The inelastic macroscopic response of concrete is

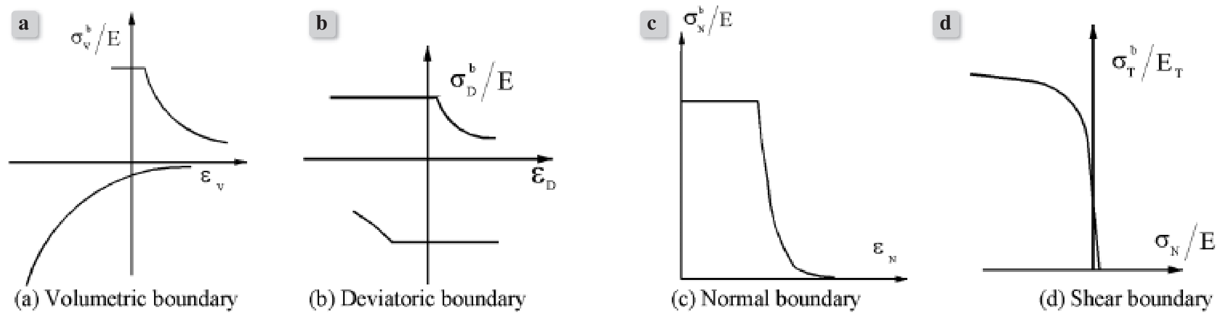

Figure 2.
Microscopic stress boundaries

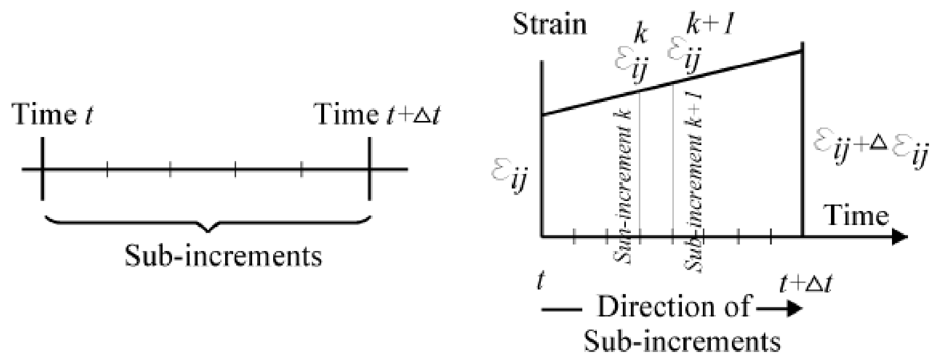

Figure 3.
Sub-increment technique for computing the incremental stress

considered to arise from microcracks initiated at the microstructural level. The concept of microscopic stress boundaries is introduced to capture the microscopic behaviour after cracking, as well as to simulate the softening behaviour of concrete [16, 3]. Figures 2(a) to 2(d) depict the microscopic stress boundary curves for the microscopic volumetric, deviatoric, normal, and shear stresses, respectively [3]. Inside the boundaries, the response is assumed linear elastic; it is governed by incremental or rate equations of the form:

$$\dot{\sigma}_V = E_V \dot{\varepsilon}_V, \quad \dot{\sigma}_D = E_D \dot{\varepsilon}_D \tag{6}$$

$$\dot{\sigma}_M = E_T \dot{\varepsilon}_L, \quad \dot{\sigma}_L = E_T \dot{\varepsilon}_L \tag{7}$$

Here, E_V, E_D and E_T represent the microplane elastic moduli. They are related to the macroscopic Young's modulus E and Poisson's ratio υ as follows [3]:

$$E_V = \frac{E}{1-2\upsilon}, \quad E_D = \frac{5E}{[(2+3\mu)(1+\upsilon)]}, \qquad E_T = \mu E_D \tag{8}$$

where μ is a parameter that characterizes the effects of damage. Along the boundaries, the various microstress-microstrain relations are presented in the work of Bažant et al. [3] are shown schematically in Figures 2(a) to 2(d).

In general, the microscopic stress components are computed separately on the various planes, which are treated independently of one another. As a result, the equilibrium condition between the microscopic stress components and the macroscopic stress tensor is not generally satisfied using the projection method. To satisfy overall equilibrium, the principle of virtual work is invoked, which leads to the following expression for the macroscopic stress tensor [15, 16, 3]:

$$\sigma_{ij} = \sigma_V \delta_{ij} + \frac{3}{2\pi}\int_{\Omega}\left[\sigma_D\left(N_{ij} - \frac{\delta_{ij}}{3}\right) + \sigma_L L_{ij} + \sigma_M M_{ij}\right] d\Omega \tag{9}$$

Numerically, this integration is carried out over a unit hemisphere Ω using an optimal Gaussian integration formula [2, 15]. This leads to an expression of the form:

$$\sigma_{ij} \approx \sigma_V \delta_{ij} + 6\sum_{N=1}^{N=m} w_N \left[\sigma_D\left(N_{ij} - \frac{\delta_{ij}}{3}\right) + \sigma_L L_{ij} + \sigma_M M_{ij}\right]_N \tag{10}$$

where m is the number of microplanes and the w_N represent the integration coefficients. The values of these coefficients for the 28-plane representative volume element of Figure 1(a) can be found in Bažant and Oh [2].

2.1. User-defined material subroutine for ADINA, Version 8.4

The microplane concrete model has been implemented as a user-supplied subroutine in ADINA to take advantage of the rich library of elements and powerful numerical tools available in this commercial finite element package.

For each increment size (time Δt), the total strain increment ($\Delta\varepsilon$) is divided into sub-increments and the microplane model is called for in each sub-increment to update the sub-increment microscopic and macroscopic stress components. This procedure for computing the incremental stress ($\Delta\sigma$) using the sub-increment strains, as can be seen in Figure 3, is recommended due to the high nonlinearities associated with the microplane model. The stress integration is performed by forward integration, where the stress increment value is updated at the end of each sub-increment. Typically, ten sub-increments are considered in the simulations.

At each integration point, one array is constructed to store 112 independent variables including 28 microscopic values defining ε_M, ε_L, ε_N and ε_D to characterize the history of the microscopic concrete behaviour. These values are updated at the end of each sub-increment. The material properties consisting of six adjustable parameters and eighteen fixed constants are specified in an array set for each integration point. The six macroscopic stress and strain components are stored in two separate arrays.

The microplane user-defined subroutine is called for all integration points to perform four types of operations during the various phases. At the beginning of the analysis the user-defined subroutine is used to initialize the variables stored at each integration point (macroscopic and microscopic stress and strain components); this is performed only once during the input phase. Usually the variables are initially set to zero. During the solution phase, the subroutine is called at each sub-increment to update the microscopic and macroscopic stress and strain components. After updating the various variables associated with each integration point, the subroutine is called to compute the tangent stiffness matrix. We have provided a special code inside the user-defined subroutine to print out the microscopic stress components (volumetric, deviatoric, normal, and shear microscopic stress components) in the output file.

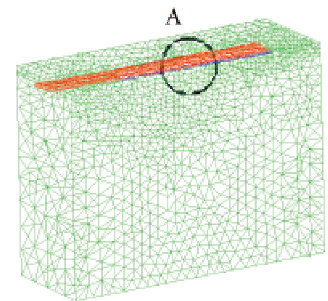

(a) FRP/concrete joint

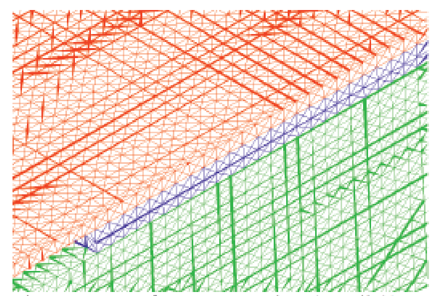

(b) Detailed mesh in the top 30 mm for concrete prism (Detail A)

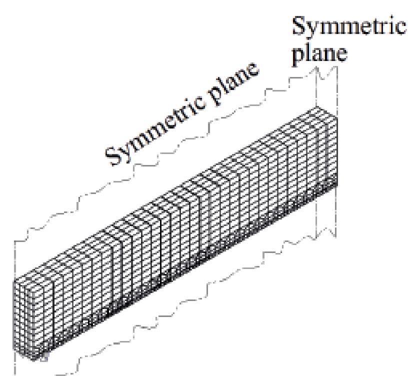

(c) FRP-strengthened concrete beams

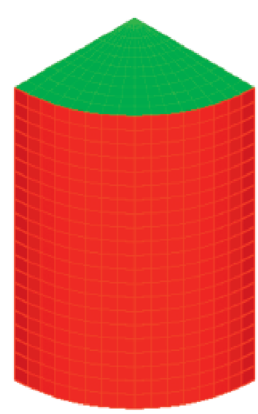

(d) Deformed shape of FRP-wrapped concrete column

Figure 4.
Finite element mesh

3. FINITE ELEMENT MODEL

For the three applications of FRP-strengthened concrete structures, 3D analyses are employed. Four-node tetrahedral solid elements with three translational degrees of freedom per node are used to represent the concrete, FRP laminate and adhesive layers in the finite element models of FRP/concrete joints. In this model, the element sizes of the concrete prism in the top 30.0 mm beneath the FRP laminates are taken as 0.5 mm cube. For the remainder of the concrete elements, the element sizes are taken from 2-5 mm cube. Two elements are taken through the depth of the adhesive layer. For the FRP laminates, the element size is taken as 0.5 mm cube. The average numbers of elements used in the analysis of FRP/concrete joints are roughly 34,000, 280,000, and 136,000 for the specimens tested by Chajes et al. [17], Bizindavyi and Neale [18], and Dai et al. [19], respectively. Figures 4(a) and 4(b) show a typical finite element mesh of an FRP/concrete joint and a detailed mesh in the top 30 mm, respectively. In both the FE models of FRP-strengthened beams and FRP-wrapped column, eight-node 3D solid elements are employed for the concrete and four-node shell elements are used for the FRP laminates.

In the application of flexurally-strengthened beams, steel reinforcement bars embedded in the concrete are described using 2-node truss elements due to their small flexural inertia compared to that of the beam section. Figures 4(c) and 4(d) show typical geometrical representations for the FRP flexurally-strengthened beam and FRP-wrapped columns, respectively. Due to the geometrical and the loading symmetry, only one quarter of the beam and one eighth of the FRP-wrapped column are modelled. Symmetrical boundary conditions are placed along the planes of symmetry. A displacement-controlled numerical procedure is used in the finite element analysis to capture the softening branch of the load-displacement curve and the post-debonding behaviour.

The orthotropy of each FRP strip is accounted for in the constitutive material properties of the corresponding elements depending on the fibre orientation. The elastic modulus in the direction perpendicular to the fibres is assumed one-tenth of that in the direction of the fibre. Generally, the debonding or rupture of the FRP laminate takes place at low stress levels in the adhesive layer; this requires no explicit consideration of a failure criterion for the adhesive layer in our simulations. Accordingly, the adhesive layers are assumed as isotropic linear elastic materials. One exception is that where the yield strength of the adhesive layer is relatively low (some specimens of Dai et al. [19]). Here the adhesive layer is modelled as an elastic-perfectly plastic material.

4. MICROMECHANICS-BASED NONLINEAR FINITE ELEMENT MODELLING OF FRP/CONCRETE JOINTS

Most studies have simulated FRP/concrete joints using plane stress elements disregarding the influence of the out-of-plane stress components on the behaviour of the bondslip model. All these analyses have adopted linear or nonlinear elasticity relations to represent the interfacial behaviour of a FRP/concrete joint [20, 21]. The FE simulations have been restricted to the plane stress assumption to avoid the high computational demands of 3D analyses. So called "meso-scale" finite element model was introduced to describe the interfacial behaviour of the top 45.0 mm of FRP/concrete joints using plane stress analysis [20, 21]. (Note that this model is called mesoscale due to the use of small element sizes rather than representing concrete at the microstructure level.) However, experimental tests on FRP/concrete joints subjected to direct shear loadings have shown 3D modes of failure in the concrete block [18]. Accordingly, in this paper complete concrete block, adhesive layer, and FRP laminates are modelled. In the following sections, the predicted ultimate load carrying capacities and local bond-slip ($\tau - s$) relationships of the FRP/concrete joints are presented.

4.1. Ultimate load carrying capacities

Experimental results of 40 specimens, carried out by different researchers, are used to validate the finite element analyses. The database is versatile in terms of geometrical characteristics and material properties of concrete, adhesive layer, and FRP composites. These 40 specimens correspond to those tested by Chajes et al. [17], Bizindavyi and Neale [18], and Dai et al. [19]. They have been chosen from the available large database because they have clear and accurate reported data for the materials used.

The comparisons between the finite element predictions with the microplane model and experimental results for all the 40 specimens, in terms of the ultimate load carrying capacities, are depicted in Figure 5. As seen in the figure, there is a very good agreement between the numerically predicted load capacities and the experimental results for all the test spec-

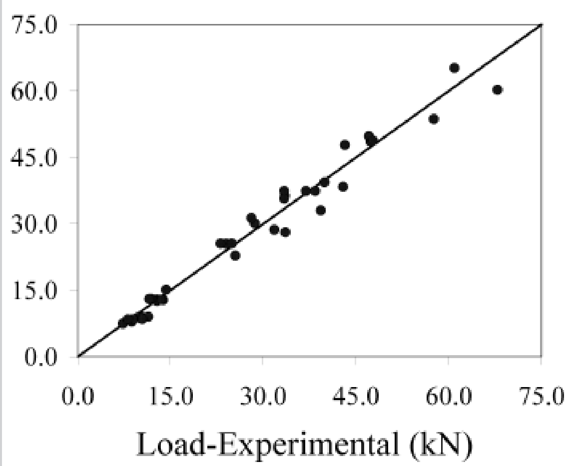

Figure 5.
Comparison between the numerical and experimental load capacities

imens. The average numerical-to-experimental load ratio is 0.98 with a corresponding standard deviation of 0.095, which indicates an excellent predictive capability of the finite element model. The scatter in the predicted results (9.5%) is within the admissible range of the direct shear test. These predictions should not necessarily be considered as unsafe in that the values do not exceed 10% over the experimental values (less than the normal average scatter for results of the FRP/concrete joint tests).

4.2. Local bond-slip relationships

In this section, the $\tau - s$ curves based on the above micromechanics-based finite element simulations are presented. These curves, for the Dai et al. (2005) set of specimens, are depicted in Figures 6(a) and 6(b). In Figure 6(a), the $\tau - s$ profiles are given at five different locations along the adhesive/concrete interface. The bond-strength τ_{max} has a value of 22.3 MPa, 7.4 MPa, 8.9 MPa, 6.3 MPa, and 4.4 MPa, respectively, at the loaded end, 2.0 mm, 4.0 mm, 6.0 mm, and 165.0 mm (the middle point) from the loaded end. The bond-slip relationships in Figure 6(a) are characterized by a residual stress with an average value around 10 to 15% of the bond strength. We observe that the slope of these relationships is almost independent of the distance from the loaded end; however, the maximum shear strength occurs at high slips (Figure 6 (a)). In Figure 6(b), the $\tau - s$ relationships are presented for various points through the depth of the concrete at the loaded end. The maximum value of the bond strength occurs at the adhesive/concrete

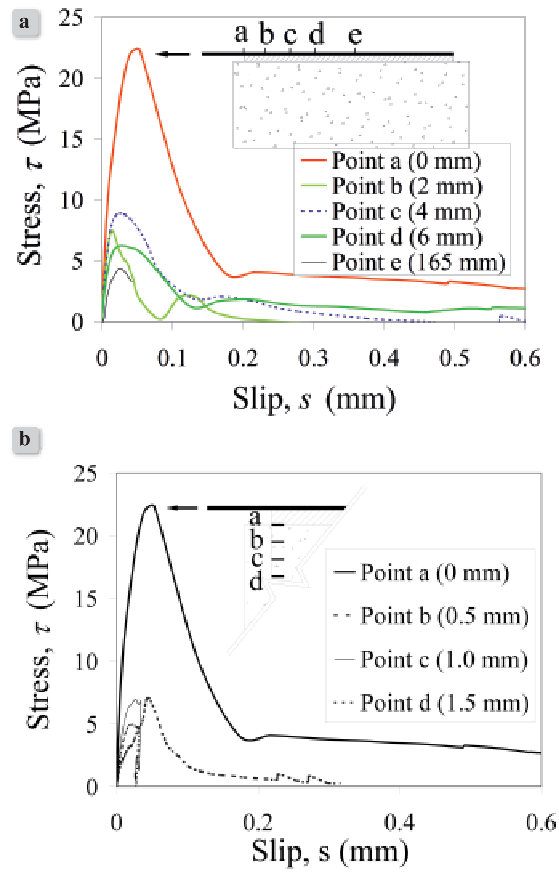

Figure 6.
Bond-slip relationships predicted using micromechanics-based FE analysis
(a) At several locations along the adhesive/concrete interface
(b) At several locations through the depth of the concrete

interface, with a value of 22.3 MPa. From Figure 6, one can observe that the bond-slip curves have the same overall shapes; however, they have different values of bond strength. This behaviour has been observed and reported in several experimental studies [22, 23, and 19]. Based on our finite element results, one can conclude that FRP/concrete joints subjected to direct shear loadings do not represent the case of a pure shear test. Because of the shear stress variation, through the depth of the concrete or along the bonded FRP laminate, normal stress components necessarily develop inside the concrete to satisfy equilibrium. Because of using the microplane constitutive relations that account for the shear nonlinearity and shear-compression interaction of the concrete, this work is the first finite element simulation that explains this peculiarity of the bond-slip profile. All the numerical analyses in the literature to analyze the debonding load of FRP/concrete joints have assumed unified bond-slip characteristics along the interface because of the implemented phenomenological concrete models [20, 21]. In fact, this assumption contradicts the experimental observations.

5. MICROMECHANICS-BASED FINITE ELEMENT ANALYSIS OF REINFORCED CONCRETE BEAMS STRENGTHENED IN FLEXURE WITH FRPS

In the literature, three approaches have been proposed to simulate debonding mechanisms in finite element analyses of FRP-strengthened concrete beams. One approach involves simulating cracking and failure of the concrete adjacent to the adhesive layer using a very fine mesh. This approach is based on very small element sizes (less than the average aggregate size of the concrete), which in certain cases may lead to the type of spurious mesh sensitivity discussed by Bažant and Planas [24]. A second approach employs a discrete crack model to represent the discontinuities due to major cracks at predefined locations, while the smeared crack model is used for the regions between these cracks [25, 26]. Although this approach is able to capture the debonding and local behaviour at the predefined locations, the predictions are dependent on the manner with which the predefined crack locations are determined and the paths that are specified for the crack propagations. In the third approach, interface elements having a specific bond–slip relation linking the FRP and concrete nodes are employed [27, 28].

In this paper, another attempt is made to capture the debonding load of FRP-strengthened concrete beams. The objective of this investigation is to assess the feasibility of using the microplane concrete model to represent the debonding behaviour of FRP-strengthened concrete beams *without* introducing an explicit interface element. With that, this paper constitutes a pioneering attempt to use the microplane model, as a concrete constitutive law, for simulating the flexural and interfacial responses of reinforced concrete beams strengthened using FRPs. Two mesh sizes in the vicinity of the FRP/concrete and steel/concrete interfaces are used to assess the effect of the mesh size on the accuracy of the results.

The specimen B-08S tested by Kotynia et al. [29] has been considered in the 3D finite element simulations. Figure 7 shows the predicted load-deflection relationships for the case where the microplane model is used to represent the concrete. Two mesh sizes are considered in this simulation. The first is a mesh of an element size of 12.5 mm along the interface, shown in Figure 4(c). A comparison between the finite element prediction using this relatively coarse mesh and experimental data in terms of the load-deflection behaviour is shown in Figure 7(a). The second numerical model consists of a refined mesh (0.25 mm along the interface). The predicted load-deflection profile for the latter finite element mesh is depicted in Figure 7(b). The finite element analysis based on the microplane constitutive law in case of the coarse finite element mesh fails to simulate the debonding phenomena.

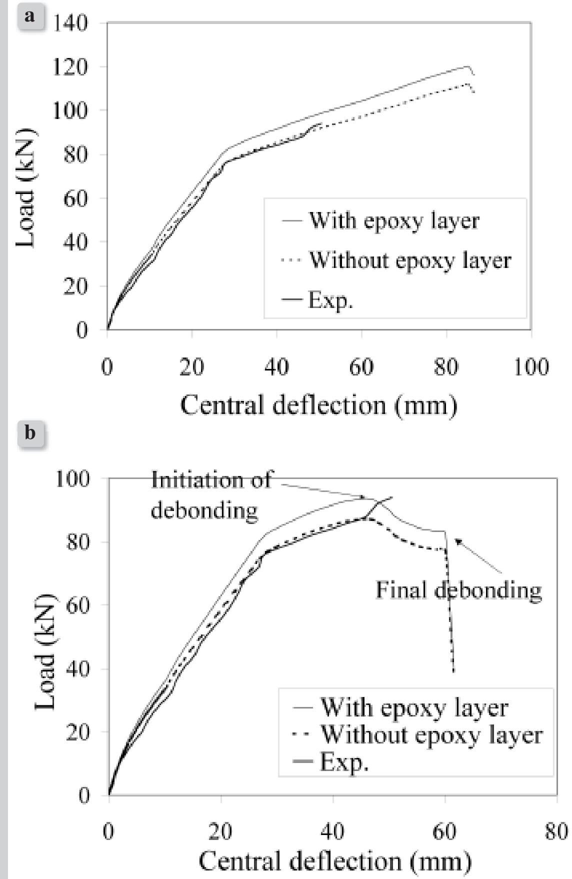

Figure 7.
Predicted load-deflection relationships of the specimen B-08S using microplane concrete model
(a) Coarse finite element mesh – 3279 elements
(b) Fine FE mesh – 762,012 and 86,911 elements for the cases with and without an epoxy layer, respectively

The problem of the finite element model with the microplane concrete law, in case of using a coarse mesh, arises from the fact that the debonding phenomenon leads to a strain discontinuity that cannot

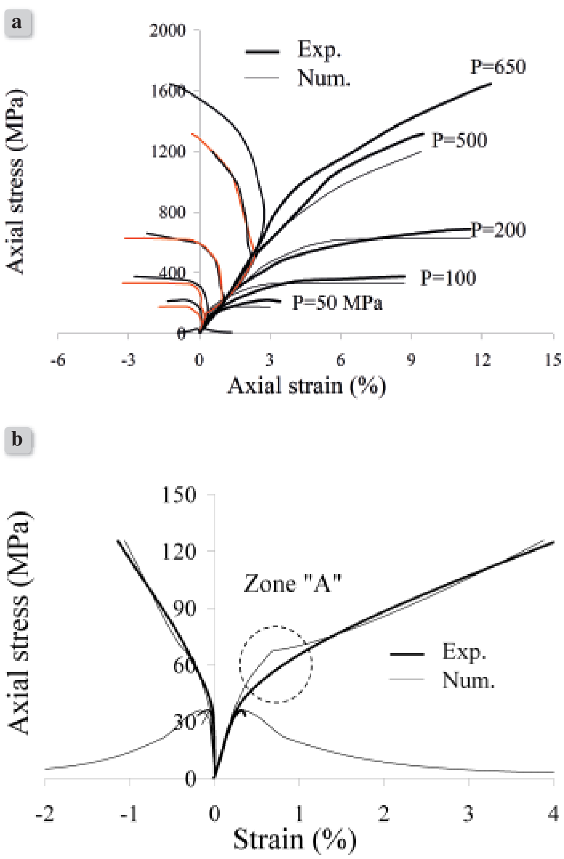

Figure 8.
Comparison between experimental and micromechanics-based predictions for concrete columns under lateral confining pressure
(a) Triaxial test under various confining pressures
(b) FRP-wrapped column

be modelled correctly with finite elements in which the strain varies continuously. The debonding causes an interfacial stress to soften with increasing cracking strain and causes a strain discontinuity due to the detachment of the laminates.

In the previous section, we showed that the finite element models with the microplane constitutive law were able to capture the debonding phenomena in case of the FRP/concrete joint subjected to direct shear loadings. To assess why the simulations based on microplane constitutive law could not capture debonding in FRP-strengthened beams, a refined finite element mesh as was previously employed to simulate the FRP/concrete joints (0.25 mm cube with a total number of 762,012 elements) has been considered along the concrete layer between the FRP and reinforcement bars. In Figure 7(b), the load-deflection relationships are shown for the refined mesh along the interface. It is clearly observed that, when using a refined FE mesh, the finite element model with the microplane constitutive law successfully captures the debonding load. The use of a small element size allows capturing the debonding load because the strain discontinuity is accounted for by considering various elements in the vicinity of the cracks.

6. MICROMECHANICS-BASED NUMERICAL SIMULATION OF FRP-WRAPPED CONCRETE COLUMNS

A survey of the literature reveals that the nonlinear finite element analyses of FRP-wrapped concrete columns are restricted to simulate the axial stress-axial strain and axial stress-lateral strain of FRP-wrapped columns. These analyses adopted two concrete constitutive laws; namely, nonlinear elastic, and elastoplastic formulations [30, 31, 8, 13, 32, and 9]. Both of these two approaches are used, whether simulating the hardening behaviour of confined concrete or the softening branch of the unconfined column. To date, there has been no unified finite element model that would describe the mechanical characteristics of FRP-wrapped concrete columns under a wide range of complex stress and strain histories. In this work, we aim to simulate the actual behaviour of such columns using microstructural finite element analyses and to introduce the first attempt to date to implement the microplane concrete model to numerically simulate the axial behaviour of such columns. The analyses in this section are carried out using two different procedures. The first is the use of the finite element analysis with a user-defined subroutine, while in the second analysis the confinement behaviour is simulated using an in-house code. This in-house code uses the microplane model to represent the concrete behaviour and the arc-length iterative technique for the numerical implementations to predict the stress–strain relationship of the column up to failure. An accurate equation correlating the axial stiffness of the FRP laminates and the lateral strain of the concrete columns to the confining pressure is incorporated in the code. The two analyses give almost the same predictions with minor discrepancies due to some numerical aspects. All details concerning the in-house code and the related formulations will be presented in the future publications.

The effect of lateral confinement on the axial stress-axial strain and axial stress-lateral strain of column is presented in Figure 8(a). In this figure, the confining pressure varies from $1.8 f'_c$ to $23 f'_c$. The figure shows the comparison between the experimental results of Gabet al. [33] and those predicted using the micromechanics-based finite element analysis. The thick lines in this figure indicate the experimental results, while the thin lines refer to the numerical predictions. In Figure 8(b) the same comparison for FRP-wrapped columns, using six layers of CFRP sheets with total width of 1.0 mm tested at University of Sherbrooke, is depicted. Based on Figure 8(a) and 8(b), it is concluded that the microplane approach accurately represents the stress–strain relationships of the concrete under several lateral confining pressures with values above around f'_c. Furthermore, the microplane concrete hypothesis is very effective in representing the softening and cracking responses of unconfined concrete as well. However, we observe that the model gives good agreement with experimental results for confining pressures greater than f'_c and there are some inconsistencies in the predictions for cases of applying confining pressures less than this value. In the application of FRP-wrapped concrete columns, we observed that the microplane model precisely simulates axial stress-axial strain relationships of FRP-wrapped columns under a relatively high confining pressure such as cases of using more than three carbon FRP sheets. When using one or two FRP sheets, the microplane model has some difficulty to represent the hardening branch of the axial stress-axial strain relationship. Similar conclusions regarding the inconsistency of the predictions using the microplane model when applying low confinement lateral pressures can be found in the work of Ghazi et al. [34], Němeček et al. [35] and Di Luzio [36].

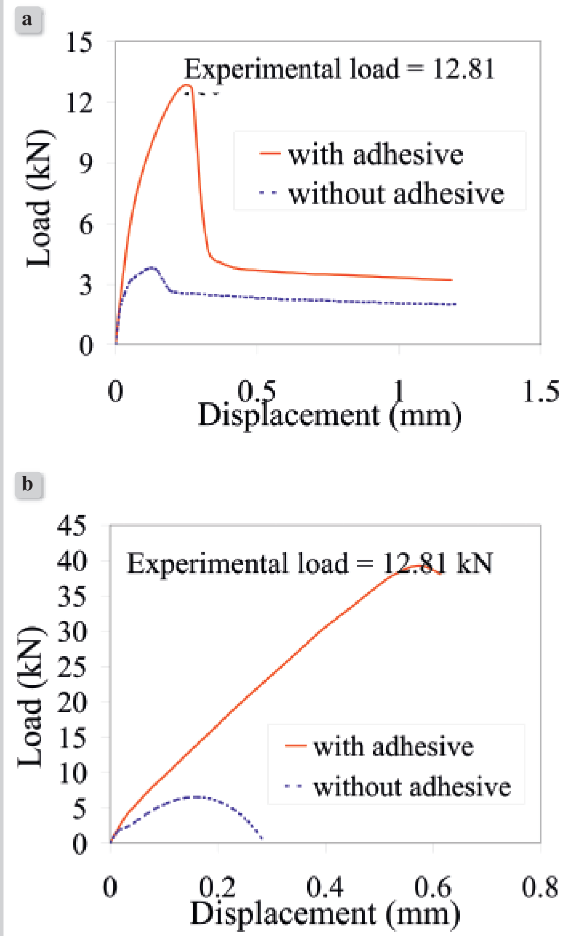

Figure 9.
Effect of the concrete constitutive law on the predictions for the direct shear test
(a) Hypoelastic concrete model
(b) Microplane concrete model

7. EFFECT OF THE MATERIAL CONSTITUTIVE LAW

Two distinct concrete models have been employed for the analyses in this section to represent the concrete characteristics; one is based on the macroscopic concrete behaviour (hypoelastic model in the ADINA software), while the other model is the micromechanics-based law (microplane approach). The objective of this investigation is to assess the feasibility of using the hypoelastic and microplane concrete constitutive relations to simulate FRP-strengthened concrete structures.

For both the FRP/concrete joints and flexural-strengthened beams, two approaches have been investigated. One considers the adhesive layer between the FRP and concrete layers, while the second analysis ignores the adhesive layer and simulates the FRP/concrete joint and flexural-strengthened reinforced concrete beams assuming full bond between the concrete and FRP nodes. We aim to assess the influence of the adhesive layers in transferring shear stresses from the FRP to the concrete, and to understand the role of the adhesive layer on the debonding phenomena. For the application of FRP-wrapped concrete column, full strain compatibility is assumed between the FRP and concrete ignoring the adhesive layer.

Figures 9(a) and 9(b) show the load-displacement relationships using the hypoelastic and microplane constitutive laws, respectively in the numerical simulations of FRP/concrete joints. Obviously, the FE

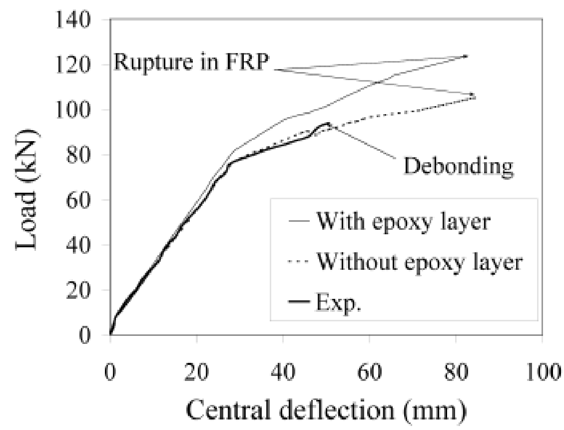

Figure 10.
Predicted load-deflection relationship of the specimen B-08S using the hypoelastic model

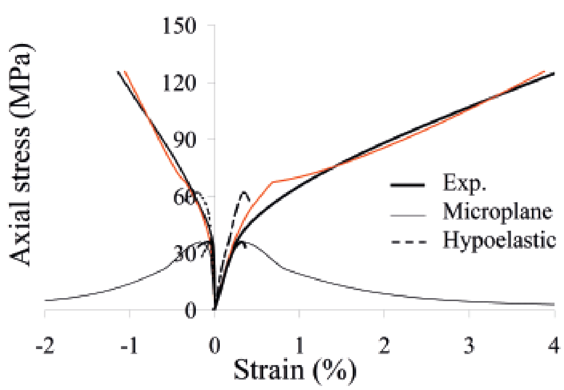

Figure 11.
Effect of the concrete constitutive law on the predictions of FRP-wrapped concrete column

model employing a hypoelastic concrete approach fails to capture the debonding load and the analysis continues until concrete crushing or rupture of the FRP occurs. By contrast, the microplane concrete model accurately captures the debonding of the FRP laminate off the concrete block (Figure 9(a)). In the phenomenological concrete model, because of the use of the smeared crack model with the phenomenological concrete constitutive law, the shear response is simulated using an empirical shear retention factor based on the tensile principal strain value regardless of the interaction of the other two principal strains. Because of the fact that the debonding mechanism depends on interfacial crack widths along the interface, it is not suitable to use a constant value for the shear modulus for cracked concrete. Generally, an accurate shear retention factor is necessary to accurately account for the shear nonlinearities of the cracked concrete and to simulate the crack width effect on the shear modulus of the concrete. The finite element study of Lu et al. [20] focused on predicting the appropriate shear retention factor to accurately capture the debonding process of FRP/concrete joints subjected to direct shear loading. In their study, the effect of four different shear retention expressions for cracked concrete were compared to identify the one that led to the most accurate predictions. It was observed that the shear retention factor has a significant influence on the ability of the finite element model to capture the debonding load. Another significant discrepancy between the predictions of the finite element model using the two concrete formulations is the shape of output bond-slip profiles. Using the microplane theory gives a bond-slip relationship that varies along the bonded length. However, the numerical predictions using the hypoelastic formulations and smeared crack model predict a constant $\tau - s$ curve along the interface. It is concluded from Figures 9(a) and 9(b) that the adhesive has a significant effect on the predicted ultimate load carrying capacity.

As far as the numerical simulations of FRP-strengthened concrete joints are concerned, Figure 10 shows the comparison between the experimental and predicted load-deflection relationships using a hypoelastic concrete relation for modelling the concrete. The same comparisons using the microplane model were previously shown in Figure 7. It is concluded that the phenomenological concrete model cannot capture the debonding load whether or not the adhesive layer is considered. This is because the hypoelastic constitutive law cannot accurately represent the interfacial shear stresses as previously proven in the application of FRP/concrete joint (Figure 9(b)). Employing interface elements with a predefined nonlinear bond-slip model overcomes this problem mentioned in the literature [28, 37]. Using Figure 10, one can notice that modelling the adhesive layer has a negligible effect on the accuracy of the simulations. However, since the model does not account for the failure criterion of the adhesive layer, the predicted load-deflection relationship is relatively stiffer than that without an adhesive layer. With that, the role of the adhesive layer in the FRP/concrete joints is different from that in FRP-strengthened concrete beams. In the earlier application, the adhesive layer transfers shear stresses from the FRP laminates to the concrete block. However, in the latter case, the flexural behaviour and the associated widening of the flexural and shear cracks govern the force transfer from the concrete beam to the FRP laminate

The hyopelastic model is seen to be unsuitable for simulating the confinement behaviour of the concrete; this is attributed to the fact that the model does not properly account for the variation of the lateral confinement pressure as the axial load is increased up to the failure of the FRP wrap. Figure 11 shows the comparison between predictions using hypoelastic and microplane relations in the application of an FRP-wrapped concrete column. This comparison is important to demonstrate the accuracy of the microplane model over that of the phenomenological constitutive relations to simulate the effect of lateral confinement on the concrete response. Obviously, the FE model employing a hypoelastic concrete approach fails to capture the hardening behaviour due to the lateral confining pressure resulting from FRP sheets. However, the microplane concrete model as previously shown in Figure 8 does simulate the behaviour.

8. CONCLUSIONS

In the first part of the paper, a nonlinear micromechanics-based finite element analysis has been developed using the microplane concrete model to simulate the behaviour of FRP/concrete joints subjected to direct shear loadings, FRP-strengthened reinforced concrete beams, and FRP-wrapped concrete columns. In the three finite element simulations, the microplane model is proven adequate in providing accurate analyses. One exception is the application of FRP-confined concrete columns under low lateral confinement pressure. In this case, some discrepancies were observed between the predicted and experimental stress-strain relationships.

In the second part of the paper, numerical comparisons between a phenomenological concrete constitutive law (hypoelastic model) and micromechanics-based model (microplane theory) to simulate the concrete behaviour in the three applications are presented. It is concluded that the microplane approach rather than the hypoelastic relation successfully simulates the nonlinearities of the interfacial shear behaviour in the application of FRP/concrete joints subjected to direct shear loadings and FRP flexurally strengthened reinforced concrete beams. The FE results indicate that the local bond–slip models are not the same along the bonded length and the associated maximum bond strength depends on the location from the loaded end. This implies that an FRP/concrete joint subjected to direct shear loadings is not the case of a pure shear test. It is clearly observed that, when using a refined FE mesh in the application of FRP-flexural strengthened reinforced concrete beams, the finite element model with the microplane constitutive law successfully captures the debonding load. The use of a small element size allows capturing the debonding load because the strain discontinuity is accounted for by considering various elements in the vicinity of the cracks. In the application of FRP-wrapped columns, the finite element analysis with the microplane concrete model accurately represents the stress-strain relationships of the concrete under several confining pressures having values above 2 f'_c. However, with low lateral confinement pressures the microplane theory needs some modifications to adequately model the concrete response.

REFERENCES

[1] *Batdorf S.B., Budiansky B.*; A Mathematical Theory of Plasticity Based on The Concept of Slip. Technical Note 1871, National Advisory Committee for Aeronautics, Washington, D.C., 1949; p.24

[2] *Bažant Z.P., Oh, B.H.*; Micro plane Model for Progressive Fracture of Concrete and Rock. Journal of Engineering Mechanics, ASCE, 111(4), 1985; p.559-582

[3] *Bažant Z.P., Caner F.C., Carol, I., Adley, M.D., Akers, S.A.*; Microplane Model M4 for Concrete. I: Formulation with Work-Conjugate Deviatoric Stress. Journal of Engineering Mechanics, ASCE, 126(9), 2000; p.944-953

[4] *Bažant Z.P., Tabbara M.R., Kazemi M.T., Pijaudier-Cabot G.*; Random Particle Model for Fracture of Aggregate or Fiber Composites. Journal of Engineering Mechanics, ASCE, 116(8), 1990; p.1686-1705

[5] *Schlangen E., Van Mier J.G.M.*; Simple Lattice Model for Numerical Simulation of Fracture of Concrete Materials and Structures. Materials and Structures, 25(153), 1992; p.534-542.

[6] ADINA; Automatic Dynamic Incremental Nonlinear Analysis: Finite Element Software, Version 8.4. ADINA R & D, Inc, Watertown, MA, USA, 2004

[7] *Chen W.F.*; Plasticity in Concrete. McGraw-Hill Co., USA, 1982; p.492

[8] *Mirmiran A., Zagers K., Yuan, W.*; Nonlinear Finite Element Modelling of Concrete Confined by Composites. Finite Elements Analysis and Design, 35(1), 2000; p.79-96

[9] *Deniaud C., Neale K.W.*; An Assessment of Constitutive Models for Concrete Columns Confined with Fibre Composite Sheets. Composite Structures, 73(3), 2006; p.318-330

[10] *Kupfer H. B., Gerstle K.H.*; Behavior of Concrete under Biaxial Stresses. Journal of Engineering Mechanics, ASCE, 99(EM4), 1973; p.853-866

[11] *Chen W.F.*; Extensibility of Concrete and Theorems of Limit Analysis. Journal of Engineering Mechanics, ASCE, 96(EM3), 1970; p.341-352

[12] *Colville J., Abbasi J.*; Plane Stress Reinforced Concrete Finite Elements. Journal of Structural Engineering, ASCE, 100(ST5), 1974; p.1067-1083

[13] P*arent S., Labossière P.*; Finite Element Analysis of Reinforced Concrete Columns Confined with Composite Materials. Canadian Journal of Civil Engineering, 27(3), 2000; p.400-411

[14] *Caner F.C., Bažant Z.P.*; Microplane Model M4 for Concrete, II: Algorithm and Calibration. Journal of Engineering Mechanics, ASCE, 126(9), 2000; p.954-961

[15] *Bažant Z.P., Prat P.C.*; Microplane Model for Brittle-Plastic Material. I: Theory. Journal of Engineering Mechanics, ASCE, 114(10), 1998; p.1672-1688

[16] *Bažant Z.P., Xiang Y., Prat P.C.*; Microplane Model for Concrete. I: Stress Strain Boundaries and Finite Strain. Journal of Engineering Mechanics, ASCE, 122(3), 1996; p.245-254

[17] *Chajes M.J., Finch W.W., Januszka T.F., Thomson T.A.*; Bond and Force Transfer of Composite Material Plates Bonded to Concrete. ACI Structural Journal, 93(2), 1996; p.295-303

[18] *Bizindavyi L., Neale K.W.*; Transfer Lengths and Bond Strengths for Composites Bonded to Concrete. Journal of Composites for Construction, 3(4), 2001; p.153-160

[19] *Dai J., Ueda T., Sato Y.*; Development of the Nonlinear Bond-Stress Slip Model of Fiber-Reinforced Plastics Sheet-Concrete Interfaces with a Simple Method. Journal of Composites for Construction, 9(1), 2005; p.52-62

[20] *Lu X.Z., Ye L.P., Teng J.G., Jiang J.J.*; Meso-Scale Finite Element Model for FRP Sheet/Plates Bonded to Concrete. Engineering Structures, 27, 2005; p.564-575

[21] *Ebead U.A., Neale K.W.*; Mechanics of Fibre-Reinforced Polymer – Concrete Interfaces. Canadian Journal of Civil Engineering, 34(3), 2007; p.367-377

[22] *Sato Y., Asano Y., Ueda T.*; Fundamental Study on Bond Mechanism of Carbon Fibre Sheet. Concrete Library International, 37, 2000; p.97-115

[23] *Nakaba K., Kanakubo T., Furuta T., Youshizawa H.*; Bond Behaviour Between Fibre-Reinforced Polymer Laminates and Concrete. ACI Structural Journal, 98(3), 2001; p.359-367

[24] *Bažant Z., Planas, J.*; Fracture and Size Effect in Concrete and Other Quasi-Brittle Materials. CRC Press LLC, USA, 1998; p.616

[25] *Yang Z., Chen J., Proverbs, D.*; Finite Element Modelling of Concrete Cover Separation Failure in FRP Plated RC Beams. Construction and Building Materials, 17(1), 2003; p.3-13

[26] *Niu H., Wu Z.*; Effects of FRP-Concrete Interface Bond Properties on the Performance of RC Beams Strengthened in Flexure with Externally Bonded FRP Sheets. Journal of Materials in Civil Engineering, ASCE, 18(5), 2006; p.723-731

[27] *Wong R., Vecchio F.*; Toward Modelling of Reinforced Concrete Members with Externally Bonded Fibre-Reinforced Polymer Composites. ACI Structural Journal, 100 (1), 2003; p.47-55

[28] *Lu X., Teng J., Ye L., Jiang J.*; Intermediate Crack Debonding in FRP-Strengthened RC Beams: FE Analysis and Strength Model. Journal of Composites for Construction, 11(2), 2007, p.161-174

[29] *Kotynia R., Abdel Baky H., Neale K. W., Ebead, U.*; Flexural Strengthening of RC Beams with Externally Bonded CFRP Systems: Test Results and 3-D Nonlinear Finite Element Analysis. Journal of Composites for Construction, ASCE, 12, 2008; p.190-201

[30] *Toutanji H.*; Stress-Strain Characteristics of Concrete Columns Externally Confined with Advanced Fibre Composite Sheets. ACI Materials Journal, 96(3), 1999; p.397-404

[31] *Spoelstra M., Monti G.*; FRP-Confined Concrete Model. Journal of Composites for Construction, ASCE, 3(3), 1999, p.143-150

[32] *Malver J., Morrill K., Crawford J.*; Numerical Modelling of Concrete Confined by Fiber-Reinforced Composites. Journal of Composites for Construction, ASCE, 8(4), 2004; p.315-322

[33] *Gobet T., Vu X.H., Malecot Y., Daudeville L.*; A New Experimental Technique for the Analysis of Concrete Under High Triaxial Loading. Journal of Physics IV, France, 134, 1999; p.633-640

[34] *Ghazi M., Attard M.M., Foster S.J.*; Modelling Triaxial Compression Using the Microplane Formulation for Low Confinement. Computers and Structures, 80, 2002; p.919-937

[35] *Němeček J., Padevět, P., Bittnar B.*; Effect of Transversal Reinforcement in Normal and High Strength Concrete Columns. Materials and Structures, 38, 2005; p.665-671

[36] *Di Luzio G.D.*; A Symmetric Over-Nonlocal Microplane Model M4 for Fracture in Concrete. Journal of Solids and Structures, 44, 2007, p.4418-4441

[37] *Abdel Baky H., Ebead U., Neale K.W.*; Flexural and Interfacial Behaviour of FRP-Strengthened Reinforced Concrete Beams. Journal of Composites for Construction, ASCE, 11(6), 2007; p.629-639